Astrocytic mechanism of glutamate modulation underlying synchronous bursting in cortical cultures

Ravi Kumar[a,c], **Yu-Ting Huang**[c], **Chun-Chung Chen**[c], **Shun-Fen Tzeng**[b], **and C. K. Chan**[c]

[a]Taiwan International Graduate Program in Interdisciplinary Neuroscience, National Cheng Kung University and Academia Sinica, Taipei, Taiwan (R.O.C) 115 ; [b]Dept. of Life Sciences, National Cheng Kung University, Tainan, Taiwan (R.O.C) ; [c]Institute of Physics, Academia Sinica, Taipei, Taiwan (R.O.C) 115

This manuscript was compiled on December 10, 2019

Synchronous bursting (SB), a collective dynamics of neuronal network, is related to brain functions. Its underlying mechanism still remains unclear. Recent studies provide sufficient evidence that astrocytes participate in synaptic transmissions. However, the role of astrocytes in SB is not yet well understood. Here, we investigated collective dynamics of astrocytes and neurons simultaneously by using cortical cell cultures developed on multi-electrode array (MEA) systems. Employing glutamate sensors (iGluSnFR) specifically expressed on astrocytes, we observed array-wide rapid rise and fall of synaptic glutamate level during SB. These glutamate traffics at synapses are likely responsible for the persistence of neuronal activities for up to seconds. We found that properties of SB events such as bursting rate and burst duration depend on the activities of GLT-1 glutamate transporters, known to majorly express on astrocytes. In addition, through genetically-encoded calcium indicator (GECI), we also observed concomitant array-wide synchronous calcium elevations in astrocytes. By including the glutamate traffics related to astrocytes, a tripartite synapse model (TUMA) was developed to conform with our experimental observations. Simulation results of the TUMA model show that astrocytes regulate synaptic transmissions by fixing the total amount of available glutamate in the pre-synaptic neuron which in turn controls the dynamics of the SB. During SB, the tripartite TUMA synapse is basically a traditional bipartite synapse with the amount of astrocyte-controlled neurotransmitters.

synchronous bursting | neuron–astrocyte interaction | glutamate transporters | multi-electrodes arrays | tripartite synapse

Synchronous firing is ubiquitous in both natural and artificial neural networks (1). These synchronous events can emerge as low frequency spiking patterns or bursts of spikes; known as synchronous bursting (SB). In our brain, SB is observed under physiological conditions (2–4); as well as in pathological states (5–8). In neuronal cultures, similar spontaneous SB (9), ictal events or seizure-like activities (10, 11) have also been widely reported. In view of the ubiquity of the occurrence of SB in both structured (in brains) and randomly connected networks (in cultures), it is highly likely that there might be a generic mechanism for SB which is insensitive to the connection topology.

In the phenomenon of SB, the neuronal system can be described by two states, the 'activated state' (during an SB) and the 'dormant state' (time between SBs). Earlier studies suggest that the activated state arises from the connectivity and excitability of the networks (12, 13). Physical connectivity does not change during the short duration of an SB. Therefore, modulation of excitability in the system can be a common mechanism for the SB observed in a variety of systems. Up to date, most of the studies have focused on the intrinsic, neuronal dynamics or neuron–neuron interactions to provide this modulation (14–17). However, another possibility is that the neuronal excitability can be modulated by the astrocytes, which greatly outnumber the neurons in the network (18–21). It is believed that they can modulate nearby neuronal activities (22, 23), form tripartite synapses (24) and exhibit calcium-excitability in response to nearby neuronal activities. Since astrocytic glutamate transporters malfunction can give rise to excitotoxicity and concomitant epileptic form of SB (25, 26), it is conceivable that the astrocytes may also modulate the SB dynamics through synaptic glutamate recycling.

One of the important findings in our understanding of synaptic dynamics in the last decades is that it can be characterized by the recycling of a conserved amount of resources as described by Tsodyks, Uziel and Markram (TUM) (27). In this bipartite synapse model, synaptic resources (glutamate) of a neuron are recycled through three states: namely the recovered, active, and inactive states. It is the recovered state which gives rise to the excitability of a neuron. Physiologically, it corresponds to the ready-to-release pool of the glutamate resource. Once released into synapse, it is known that both neurons and astrocytes can uptake the glutamate from the synapse (28). Presumably, if the astrocytes can take part in the recycling process, they should have a significant impact on the modulation of the excitability of the neurons. Since majority of glutamate is uptaken by the astrocytes, converted to

Significance Statement

Synchronous bursting (SB) in groups of interconnected neurons is a hallmark dynamics of functional neuronal circuits. This study shows that SBs are, in fact, manifestations of glutamate dynamics at synapses and its trafficking is orchestrated by neuron–astrocyte tripartite interactions through astrocytic glutamate transporters (GLT-1). Experimentally we show that the features of SB in cultured cortical networks depend on GLT-1 function. By including the GLT-1 mediated glutamate recycling, our tripartite synapse model clarifies that astrocytes modulate the amount of available glutamate at presynaptic neurons via multiple timescale depression mechanisms which in turn govern the SB patterns. Our results show that, at least for SB, the traditional bipartite synapse can still be a good description if astrocytes-dependent glutamate content is taken into account.

Authors declares no conflict of interest.

[1]R.K., Y.T., S.F., C.K. designed research; R.K. performed the research; R.K., Y.T. analyzed the research of this work; C.C developed the simulation, R.K., C.K. wrote the paper.

[2]To whom correspondence should be addressed. E-mail: ckchan@gate.sinica.edu.tw

glutamine, transported to neurons and followed by conversion back to glutamate (glutamate-glutamine cycle)(29), the time scale for the astrocytic glutamate recycling pathway should be much longer than that for the pre-synaptic neuronal pathway. One possible consequence of this difference in time scales of the two pathways is that multiple-time-scale depression in the SB can be mediated by astrocytes. In fact, recent finding by Murphy-Royal et al. (30) shows that astrocytic GLT-1 glutamate transporters can dynamically modulate synaptic events by regulating synaptic glutamate. Also, experiments with DHK (GLT-1 inhibitor) on cortical cell cultures by Huang et al. (31) have also shown to alter the period of SBs. These findings give strong support to the notion that SB could be consequence of astrocyte-mediated glutamate modulation in response to neuronal dynamics.

With the picture of astrocytic glutamate recycling above, we hypothesized that the glutamate-transporter (GluT) system of the astrocytes plays a pivotal role in SB modulation. We tested this hypothesis by both experiments as well as simulations. For the experiments, glutamate transporters were targeted in cortical cultures developed on multi-electrode array (MEA). Combining astrocyte-specific fluorescent probes with MEA, we could monitor the responses from neurons and astrocytes simultaneously. Our setup with controlled external environment makes it possible to target the two cell types specifically using pharmacological tools. To test the validity of our idea of astrocytic modulation of SB, we developed a tripartite synapse model to include astrocytes in the glutamate recycling process. We found that results from both our experiments and simulations were consistent with our hypothesis. Specifically, the excitability of the neurons were modulated by the GLT-1 transporters. Different aspects of the SB, such as the burst duration and bursting frequency, were modified when the timescale of the transporter's activity were altered. The forms of SB were found to be governed by the amount of glutamate residing in astrocytes.

Results

Active and dormant states in cortical cultures. Neurons in cortical cell cultures develop into self-organized networks forming recurrent connections (Figure S2). At the same time, astrocytes also develop and extend their processes forming their own complex network, at the vicinity of neuronal network. Functionally, the neurons exhibit a wide range of spontaneous firing patterns (9) during their course of development. Typically, after three weeks of age neuronal connections become functionally mature, and the array-wide firing patterns turn stable. Each active electrode of MEA generally display two patterns of neuronal activities: either bursts of spikes followed by isolated spikes (ch#2,3,7,9,10,14 in Figure 1A), or only bursts of spikes (ch#1,4,5,6,8,11,12,13). Aligning the temporal activities in all the electrodes, the overall array-wide firing dynamics thus appears as either asynchronous or synchronous firings in a network. A distinction between synchronous bursting and asynchronous spiking events can be made by generating inter-spike interval (ISI, time interval between successive discharge) return map (Figure 1B). Electrodes which exhibit only synchronous events, their ISI return map show single cluster lying within the range of 2–250 ms. Whereas, electrodes which also show asynchronous firings, display additional clusters of ISI distributed in the interval between 1–10 sec.

We will refer to the synchronous-discharge state of network as the 'activated state', since all neurons collectively remain active during this state (Figure 1C). Within an activated state a network exhibits different kinetics, as shown in the firing-rate time-histogram (FRTH) plot. FRTH was generated by summing the total number of array-wide action potentials detected in a 5 ms bin size. A generic SB's kinetic structure consists of the initiation, maintenance, and termination phases (Figure 1C, bottom). Initiation of SB occurs by assembly of neuronal activities at an exponential rate (32). Post-assembly of neuronal firings, array-wide firing reaches a peak level then gradually decays to the extent where all neuronal spikes ceased completely. By taking reciprocal of the ISI ranges stated above, it can be seen that the firing rate in single electrode during the activated state can range between 10-500Hz. After termination of the SB, the network maintains a period of quiescence for several seconds and regains its basal firing activities until next SB occurs. We will refer to the time between the termination and the initiation of the next SB as the 'dormant state' of the network. During the dormant state some neurons may still exhibit spontaneous firings at a rate within the range of 0.1-4Hz.

Synaptic glutamate is regulated during active and dormant states. Firing dynamics observed in SB involves fast recurrent excitation of AMPA and NMDA receptors by synapse-released glutamate(33, 34). Previous studies indicate that most of the synaptic glutamate(≈80%) is uptaken by astrocytic processes through GLT-1 transporters while only a smaller portion is directly uptaken by the neurons (35, 36). This distinction is due to the difference in the number of transporter expressions on the membranes of the two cell types. We performed a qualitative check on GLT-1 expression in our sample cortical cultures. Confocal imaging, revealed a highly clustered expression of GLT-1 (see Figure S2) around hub-like clustered neuronal bodies. A previous study (37) has shown these neuronal hub structures to be composed of organized synaptic clusters formed by assembly of presynaptic, postsynaptic and dendritic structures. Observation of intense GLT-1 expressions implies high glutamate activities at these locations. Our goal was to detect glutamate dynamics during SBs in the immediate surrounding of the astrocytes. Therefore, we employed glutamate sensors genetically expressed on astrocytic-membrane facing extracellular space.

Astrocytes in developing cortical cultures were infected with adeno-associated viruses expressing GFAP-targeted intensity-based-glutamate-sensing-fluorescent-reporter (iGluSnFr) (38) (See material and methods in SI for details). This approach has been previously shown to indicate the kinetics of glutamate clearance by astrocytes (39). Therefore, we implemented this method for evaluating GluT activities during SBs. Within two weeks (post-infection), fluorescence signals from astrocytes were detectable. Simultaneous recording of MEA and whole field synaptic glutamate imaging, revealed sharply elevated iGluSnFr signals associated with SB events recorded with MEA(Figure 2A). Its kinetics almost overlapped with the time course of network's activated state. Evidently, the sharp rise in glutamate signal was due to synaptic releases of glutamate during intense burst firings by neurons. Notably, the glutamate level rapidly decayed back to baseline level immediately towards the termination of the SBs(Figure 2B). Detected iGluSnFr signal continued to remain at its baseline

level until the next SB occurred. The time taken for the decrease of glutamate from its maximum level to half during SB was defined as τ_{half}. The glutamate decay time τ_{decay} (assuming exponential decay function(39)) was computed as $\tau_{\text{half}}/\ln 2$ (Figure 2C) to reflect the glutamate clearance time by the astrocytes. In our culture system, the decay time was found to be distributed around 0.26±0.11 s (N=8 cultures).

SB dynamics are modulated by GLT-1 glutamate transporters. To gain further insights on the role of glutamate transporters in SBs, we used pharmacological tools to dissect their contribution. Adding GluT-specific inhibitor drugs resulted in dramatic change in firing and bursting patterns(Figure 3A-B). Inhibition with DL-TBOA resulted in two-folds increase in array-wide firings (Table 1, Figure S4). Still there was no significant change in SB frequency. The SB duration was increased nearly 2.5 times. The level of array-wide spiking activities during SBs was quantified as SB index (ranging between 0 and 1, see SI for more information). Our cultured networks usually displayed an SB index of ≈0.8 in their reference recordings. DL-TBOA treatment significantly increased SB index. We also observed a rearrangement effect of firing activities in different samples. Although all networks showed consistent increase of firing activities after DL-TBOA addition, a range of change in SB duration was observed across samples. Networks which showed small increases in burst duration after the drug treatment, showed increased frequency of SB compared to their reference. Whereas, networks that displayed big increase in burst duration, showed a decrease in SB frequency. Specific inhibition of GLT-1 with DHK reproduced the effects similar to DL-TBOA treatment. The only difference was found in the SB index of the networks after drug treatment. Contrary to DL-TBOA effect, DHK addition resulted in increased asynchronous state firings which significantly reduced the burst index (Table 1, Figure S5). On the other hand, augmenting GLT-1 function with GT949, a positive allosteric modulator (PAM) drug, significantly decreased array-wide firings without affecting SB frequency and SB index. The duration of SBs became shorter than their reference, a consequence likely due to reduced firing activities (Figure 3C, S6). These results indicate that the clearance mechanism by GLT-1 acts as a major restoring force during SBs by effectively controlling the amount of glutamate in synapses.

SBs are not terminated by inhibition. Inputs from the inhibitory sub-networks are known to control the excitability of neurons. It is the interaction between the two which is believed to regulate the flow of information through the network as well as shape network activities (40–43). To gain insight on the contribution of inhibitory inputs in SB, cortical networks were treated with bicuculline (Bic, GABA antagonist, 10 μM) to suppress the fast inhibitory effects of γ-aminobutyric acid (GABA). After bicuculline addition, the SBs became more periodic (Figure 3E-F). Networks in disinhibited state also often displayed reverberatory activities (sub-bursts) within each SB event similar to previous report(44). Asynchronous activities were almost abolished while SBs were more prominent, with rather clearly-maintained active and dormant phases. The observation that networks did not fire endlessly and stop until there is no more activity after bicuculline treatment, show that termination of SBs do not depend on excitatory-inhibitory interactions.

Table 1. Pharmacological targeting glutamate transporters alters SB statistics

Drug treatments	Firing rate (spikes/s)	SB rate (minute^{-1})	SB duration (s)	SB index (0-1)
1. Ref	25±13	6±5	0.28±0.09	0.75±0.12
+ DL-TBOA	50±30, **	5±4, n.s	0.72±0.44, ***	0.84±0.11, *
	n=13	n=16	n=16	n=13
2. Ref	26±8	6±5	0.34±0.17	0.84±0.12
+ DHK	46±13, ***	6±6, n.s	0.66±0.39, **	0.67±0.18, **
	n=11	n=11	n=11	n=10
3. Ref	29±14	5±2	0.27±0.12	0.80±0.16
+ GT949	15±10, ***	4±2, n.s	0.18±0.06, *	0.83±0.09, n.s
	n=14	n=11	n=9	n=12

Summary of the changes in array-wide neuronal activities from reference (Ref) after pharmacological treatments with glutamate transporter inhibitors; DL-TBOA(10μM), DHK(200μM) or selective augmentation of GLT-1 glutamate transporter with PAM (positive allosteric modulator) drug GT949(10μM). Statistical tests: paired t tests, significance with Ref as baseline was defined as *p<0.05, n denotes number of cultures.

Analyzing the firing patterns, cultures treated with bicuculline showed significant increase in firing rate (Table 2). After disinhibition, networks engaged only in synchronous activities (burst index ≈ 1). Disinhibition also resulted in significant increase in the duration of SB while maintaining similar SB frequency compared to reference. To validate the role of GLT-1 in mediating SB dynamics in disinhibited state of cortical networks, we also pharmacologically manipulated GLT-1 transporters. Further addition of DHK did not affect the overall firing rate or the SB index but induced a re-organization of the firing events into shorter duration with higher frequency of bursting (Figure 3E). These effects were reversible as observed after washout of the drugs (see Figure S7–S8). Adding GT949 in the disinhibited networks decreased the overall network firing activities significantly while maintained the high synchronicity caused by disinhibition (Figure 3F). Under the influence of GT949, burst duration was significantly shorter, without affecting the SB frequency (Table. 2).

Astrocytes display SB-associated synchronous calcium activities. Previous studies have reported astrocytic calcium sensitivity towards synaptic glutamate activities (45). However, its role in synaptic events still remains unclear. We further probed calcium activities in astrocytes in spontaneously bursting cortical networks. Cultures were expressed with genetically encoded calcium sensors (cyto-GCaMP6f) specific to the astrocytes. GCaMP6f imaging revealed asynchronous local calcium elevation as well as synchronous calcium elevations (SCEs, Figure 4A). We noticed that, the sequence of astrocytic activation during the global calcium elevation was not random. A hierarchy in the recruitment of calcium was consistently observed. This was likely due to an existence of a stable subset of privileged neurons whose spiking activities reliably increase before the onset of global SB (32). Combining MEA and calcium imaging, temporal activities from the two cell types were recorded simultaneously. Consistently, we observed that SCEs always emerged towards the end of longer persisting SBs (Figure 4B). Note that during the SCE in astrocytes, neuronal ongoing activities were completely abolished. Neurons resumed their basal activity level shortly after decay of SCE in astrocytes. Importantly, only SBs persisting long enough

(>500 ms) were followed by the astrocytic SCE. Since SBs result in large glutamate transient at synapses globally, this transient is likely to triggered collective activation of astrocytic metabotropic glutamate subtype 5 receptors(46). A positive correlation was indeed found between the duration of SB in neurons and its concomitant SCE in astrocytes. To validate whether glutamate released by the SBs were responsible for SCE in astrocytes, cultures were treated with riluzole (glutamate release inhibitor, 10 μM). Treatment with riluzole resulted in suppressed neuronal activities with complete abolition of SBs and associated SCEs (Figure S9). Although neurons maintained some asynchronous firings, no astrocytic SCE was observed after addition of riluzole, indicating SB dependency of synchronous calcium activities in astrocytes.

Simulation results. The description of firing and bursting patterns obtained from MEA experiments show how the dynamics of SB changes under various conditions. We used these firing patterns as input to obtain relevant parameters for our tripartite synapse TUMA model. This model describes how glutamate gets relocated to different parts of a tripartite synapse. For details, please refer to the supplementary information (SI). The essentials of this model can be understood from the schematic diagram shown in Figure 5A. The amount of glutamate (expressed as fractions) in the system can be in X (ready-to-release pool), Y (activated state; producing EPSC), Z (pool of glutamate uptaken from the synapse), and A (glutamate uptaken by astrocyte). Similar to the TUM model(27), we implemented conservation of glutamate in the tripartite synapse; with $X + Y + Z + A = 1$. The glutamate transporters targeted in this study are related to the two uptake time scales in TUMA synapse; $\tau_{\rm nu}$ (neuronal uptake) and $\tau_{\rm au}$ (astrocytic uptake). The values of $\tau_{\rm nu}$ and $\tau_{\rm au}$ were obtained and fixed in a manner to match the simulated firing patterns with the experimental observations. These time constants and the model mechanism were the basis of our understanding on how glutamate dynamics control the properties of SB.

Synchronous bursting events. Figure 5C shows the raster plot of typical noise-induced synchronous firing events in 100 neurons randomly connected through TUMA synapses. The time course of X, Y, Z, and A during the SB events are also shown in the figure. Simulation parameters (see Table S1) were chosen such that the firing patterns were similar to experimental firing patterns (Figure 5B) and consistent with published values(47, 48). Before the onset of SB, the fraction X was at its maximum, while Z was at its minimum. Most of the changes in X were supplied from Z. Once the SB is triggered, a steep rise in Y happens similar to our experimental observations (Figure 2). One remarkable feature shown in the figure is that during an SB, changes in X and Z were large while only very small changes occurred in A. These changes in A during SB were small because of the slow process for A to turn into Z. If this later process was much faster, one would expect bigger changes in A during an SB event.

Slower astrocytic uptake increases SB rate and duration. The effects of the astrocyte uptake time scale on the properties of SB are shown in Figure 5D(a–b). It can be seen that an increase in $\tau_{\rm au}$, from 200 ms to 300 ms, caused a substantial increase in the overall firings, bursting rate, bursting duration and burst index (Figure 5E). This effect should be similar to the inhibition of the astrocytic uptake by DHK treatment in our experiments. These increases reflect the fact that more glutamate becomes available in the synapse while A gets smaller. Figure 5D(a–b) shows that A remained relatively constant during the SBs however its mean value was sensitive to the value of $\tau_{\rm au}$. A change of $\tau_{\rm au}$ from 200 ms to 300 ms decreased A from 0.71 to 0.66. A further increase in $\tau_{\rm au}$ would decrease A to an even smaller value and vice versa. These findings were consistent with the schematic picture that A works as a temporary storage for the glutamate and can modulate the amount of available glutamate in the synapse(49). With the parameters used to reproduce experiment observations, the simulation revealed that A remains relatively constant and sets the amount of glutamate available to X.

Table 2. Comparison of SB statistics under GLT-1 specific treatments in disinhibited state of cortical networks.

Drug treatments	Firing rate (spikes/s)	SB rate (minute^{-1})	SB duration (s)	SB index (0-1)
1. Ref	34±22	7±5	0.28±0.19	0.86±0.12
+ Bic	82±48, *	7±4, n.s	0.85±0.49, *	0.99±0.01, *
+ DHK	97±31, n.s	21±16, *	0.58±0.35, *	0.99±0.01, n.s
	F(2,10)=21.19, ***	F(2,10)=10.26, **	F(2,8)=12.21, **	χ^2 (2,9)=9.8, **
2. Ref	27±17	5±2	0.35±0.24	0.84±0.12
+ Bic	60±42, *	8±4, n.s	0.73±0.42, ***	0.99±0.01, **
+ GT949	12±08, **	5±3, n.s	0.17±0.05, **	0.99±0.02, n.s
	F(2,9)=14.88, **	F(2,8)=2.43, n.s	F(2,9)=16.64, **	χ^2 (2,8)=12.67, ***

Summary of the changes in array-wide neuronal activities from reference (Ref) to pharmacologically disinhibited state (Bic, 10μM) followed by manipulation of GLT-1 glutamate transporters with DHK (200 μM) or GT949 (10 μM). Statistical tests: repeated measures one-way ANOVA (F) and non-parametric Friedman test (χ^2), significance *p<0.05.

SB can be produced by a fixed A. A remains nearly constant during SBs for different values of $\tau_{\rm au}$ as shown in Figures 5D, a–b. These results suggest that astrocytes do not directly take part in the generation of an SB. Still, their role is to set the amount of available glutamate in the synaptic dynamics. By fixing A as a constant (Figures 5D, c–d), it can be seen that SBs were generated similar to the experiments, indicating that the dynamics of A is not important for the generation of SB. By fixing A, our tripartite synapse was in fact reduced to a bipartite synapse. As a bipartite (TUM) synapse is governed by $X+Y+Z=1$, fixing A was equivalent to $X+Y+Z=1-A$, were $1-A$ became another constant <1. This finding strongly suggests that the main role of astrocytes in generation of SB is to limit the amount of glutamate available in the bipartite synapse. The availability of glutamate then governs the firing patterns in SBs.

Slower transformation of A to Z decreases SB rate and duration. According to our TUMA model, the amount of glutamate in the A state can be varied either by varying $\tau_{\rm au}$ or τ_g. Here τ_g represents the timescale for glutamate-glutamine cycle which is followed by astrocytic glutamate uptake. Previous research have shown the importance of this cycle for the generation of bursting activities in neurons (50, 51). Figure 5E shows network bursting statistics under combinations of different $\tau_{\rm au}$ and τ_g. Although τ_g has been used as an overly simplified representation of multiple processes that occur in the course of glutamate transport from astrocytes to neurons in this

study, these simulation results provide an estimated range of τ_g within which this recovery may take place. From the data pooled from our cortical culture experiments, the reference SB statistics were found to be in the following ranges: array-wide firing rate (≈26 spikes/s), SB duration (≈0.29 s), SB index (≈0.82), and SB rate (≈5 SBs/minute). Also, the glutamate decay time (τ_{decay}) measured across networks was found to be ≈0.26 s. In order to align with these values, it can be seen from Figure 5 that τ_g should lie around 30s range. Furthermore, the effect of blocking astrocytic glutamate-glutamine cycle on bursting activities in the previous reports(50, 51) comply with effect of increasing τ_g.

Discussions

Experimental evidence across brain regions show that vesicle release can occur at the rate of 0.3–70 vesicles per spike (52, 53), each vesicle carrying about 4,000 glutamate molecules (54). Now, considering a presynaptic firing rate of 100 Hz, a synapse can witness 1.2×10^5–2.8×10^7 molecules of glutamate turnover per second. Hence, an SB event involving millions of synapses can cause a massive rise in synaptic glutamate level. Their dwelling time in the synaptic region is very likely to dictate the post-synaptic response duration. Therefore, a gating system is necessary to limit the extent of glutamatergic excitation and thus limit the persistence of firing events. Since the majority of glutamate re-uptake happens via astrocytic GLT-1 GluTs, they qualify to be an important regulatory body during synchronous neurotransmissions. Indeed, our experimental and simulation results show that SBs observed in cortical cultures are associated with re-distribution of a conserved amount of glutamate in different forms and locations.

The main finding of our experiments and simulations is that the amount of glutamate in astrocytes govern the collective dynamics in SB. Based on our modeling, the effects of A on the phenomenon of SB can be divided into the following phases:
Initiation and positive feedback: In the dormant phase of the network, the number of asynchronous release increases(see Figure 1) before SB. These releases come from the noise-induced release of X which build up slowly during the dormant state. If these release events become large enough and the connectivity in the network is also high enough, action potentials gets triggered in some neurons. Once this happens, more glutamate gets released by these action potentials triggering more neurons to fire due to recurrent connections in the system. Consequently, this positive feedback then triggers a system-wide firing events.
Maintenance of burst (activated phase): The positive feedback can be maintained as long as there is enough X to be released to trigger further action potentials. Depending on the system parameters (A level), sub-burst in the form of reverberations can also be possible because of the interaction between synaptic facilitation and depression in the TUM mechanism. One would expect reverberations to be more easily observed in a system with only excitatory inputs similar to experiments with bicuculline. This is because for systems with both inhibitory and excitatory inputs, there should be a wider and weaker distribution of input currents to the neurons. Intuitively, system with higher X (lower A) should have longer bursting duration because it will take longer for X to deplete to a certain threshold. Indeed, we see from both experiments (Table 1) and simulations (Figure 5D) that SB duration decreases with the amount of glutamate in the astrocyte.
Termination of burst: During the activated state of SB, the ready-to-release glutamate molecules (X) are constantly being transformed into Z, via multiple timescale processes, which will then be turned slowly back to X controlled by another long time constant. Due to overall slower recovery mechanism, X is not replenished fast enough from Z. The action potential triggered release from the pre-synaptic cell will be then too small to elicit action potentials at the post-synaptic cell. In this scenario, the positive feedback can no longer be sustained and the bursting will stop.
Dormant phase (deactivated phase): Once the system is in the dormant state, system-wide firings stop and there are only isolated spikes created by noise-driven releases. During this phase, X can slowly recover from Z. As X increases, the amount of noise-driven-released glutamate will also increase, raising the probability of triggering a system-wide depolarization.

In our TUMA model, we assumed that the amount of glutamate is conserved within the tripartite synapse. As we have shown in our simulations (Figure 5), the effect of astrocytes in our tripartite synapse is to control the level of glutamate available to neurons. During the different phases of SB, there is very little change in A. In fact, one can even fix A and still obtain qualitatively similar collective bursting patterns. In this latter case, we are back to the traditional bipartite synapses (TUM model with $X+Y+Z$ being a constant but less than one). The role of astrocytes here is to set the overall level of A through the two processes of uptake from Y and transforming A to X. Therefore, even if there is a violation of the conservation, it will not invalidate our conclusion as long as the overall A is fixed to a certain level.

Termination of SBs were found to be independent of inputs from inhibitory sub-networks. Pharmacologically removing the inhibition, with addition of bicuculline, although enhanced firing probability of networks resulting in longer SBs, the SBs were eventually terminated and followed by dormant states. Our simulation shows that the dormant state is in fact the network's refractory period during which there is a slow recovery of glutamate in X. During the recovery, the neuronal network could not generate another SB due to insufficient glutamate available in the presynapse. This recovery process can be regarded as a slow negative feedback mechanism, which effectively controls the occurrence of SBs.

During the activated state, it is clear that there are SCEs in the astrocytes (Figure 4). Its contribution was unaccounted for in our TUMA model. From Figure 4B, the SCEs in astrocytes appear to have a role in the termination of SBs. For such an observation, there are multiple possible scenarios: First, calcium elevation may trigger astrocytic transmitters ('gliotransmitter') release into the synapses which may suppress the persisting neuronal activities(55). Two possible candidates are ATP/adenosine(46, 56) and nitric oxide(57) which have been reported to suppress hetero-synaptic activities. Second, the SCE may also be associated with recruitment of additional astrocytic GluTs for more rapid uptake of glutamate from the synapse. These two processes may also occur simultaneously. In a contrasting scenario, astrocytic concomitant SCE response could be positive feedback mechanism associated with increased glutamine transport to the neurons or calcium-induced glutamate release(58). It required further

experiments to test these hypotheses.

With the picture described above, the SB phenomenon can be considered as a generic property of a neuron-astrocyte system. No special circuits or burster neurons are needed for its generation. We show that such collective dynamics is an outcome of synergistic interactions between neurons and astrocytes as demonstrated in the TUMA model. The most important finding in our work is that, the firing and bursting patterns of the neurons are governed by the amount of glutamate in the astrocytes (A). It is possible that different regions of brain can have different amount A in the astrocytes locally, allowing different firing and bursting patterns at different brain regions. In this sense, the astrocytes are modulating the bursting of neurons in the network.

Finally, we like to point out that neurological disorders such as seizure-like epilepsy and even behavioural changes can be associated with GLT-1 malfunction(59–63). Our study contributes to the understanding of how altered uptake mechanisms can affect a network's firing and bursting activities, which are representative of brain circuit's functions. In the astrocyte targeted experiment of Bechtholt-Gompf et. al. and John et. al. (61, 63), a depression-like behaviour was induced in rats by DHK treatment; the same drug used here. If we extend our findings to understand their observations, it seems that the increase in firings induced by the DHK are the origin of such changes. In terms of our model, this is just a decrease in the level of glutamate in the astrocytes (the A state). This last observation is consistent with the current view that astrocytes can be important in shaping the behaviour of animals(64).

Materials and Methods

All samples from animals were prepared according to the guidelines approved by Academia Sinica IACUC (Protocol: 12-12-475). All pharmacological experiments and simultaneous recordings of MEA and iGluSnFr-glutamate imaging/ GCaMP6f- calcium imaging were performed on cultures (age $>$ 20 DIV) inside home-made incubation chamber maintained at 5% CO_2 - 95% air at 37°C. More details on the materials and methods implemented in experiments as well as complete description of the TUMA model, simulation methods details and the simulation parameters (Table S1) used in this work are provided in the supplementary information file.

ACKNOWLEDGMENTS. This research work was supported by Taiwan's MOST funds: 105-2112-M-001 -017 -MY3 and 108-2112-M-001 -029 -MY3.

1. Arenas A, Díaz-Guilera A, Kurths J, Moreno Y, Zhou C (2008) Synchronization in complex networks. *Physics reports* 469(3):93–153.
2. Tallon-Baudry C, Mandon S, Freiwald WA, Kreiter AK (2004) Oscillatory synchrony in the monkey temporal lobe correlates with performance in a visual short-term memory task. *Cerebral cortex* 14(7):713–720.
3. Axmacher N, Mormann F, Fernández G, Elger CE, Fell J (2006) Memory formation by neuronal synchronization. *Brain research reviews* 52(1):170–182.
4. Krahe R, Gabbiani F (2004) Burst firing in sensory systems. *Nature Reviews Neuroscience* 5(1):13.
5. Traub RD (2003) Fast oscillations and epilepsy. *Epilepsy currents* 3(3):77–79.
6. van der Stelt O, Belger A, Lieberman JA (2004) Macroscopic fast neuronal oscillations and synchrony in schizophrenia. *Proceedings of the National Academy of Sciences* 101(51):17567–17568.
7. McAuley J, Marsden C (2000) Physiological and pathological tremors and rhythmic central motor control. *Brain* 123(8):1545–1567.
8. Hutchison WD, et al. (2004) Neuronal oscillations in the basal ganglia and movement disorders: evidence from whole animal and human recordings. *Journal of Neuroscience* 24(42):9240–9243.
9. Wagenaar DA, Pine J, Potter SM (2006) An extremely rich repertoire of bursting patterns during the development of cortical cultures. *BMC neuroscience* 7(1):11.
10. Avoli M, et al. (2002) Network and pharmacological mechanisms leading to epileptiform synchronization in the limbic system in vitro. *Progress in neurobiology* 68(3):167–207.
11. Adams BE, et al. (2011) Seizure-like thalamocortical rhythms initiate in the deep layers of the cortex in a co-culture model. *Experimental neurology* 227(1):203–209.
12. Cohen I, Miles R (2000) Contributions of intrinsic and synaptic activities to the generation of neuronal discharges in in vitro hippocampus. *The Journal of physiology* 524(2):485–502.
13. Izhikevich EM (2000) Neural excitability, spiking and bursting. *International journal of bifurcation and chaos* 10(06):1171–1266.
14. von Krosigk M, Bal T, McCormick DA (1993) Cellular mechanisms of a synchronized oscillation in the thalamus. *Science* 261(5119):361–364.
15. McCormick DA, Contreras D (2001) On the cellular and network bases of epileptic seizures. *Annual review of physiology* 63(1):815–846.
16. Sirota A, et al. (2008) Entrainment of neocortical neurons and gamma oscillations by the hippocampal theta rhythm. *Neuron* 60(4):683–697.
17. Penn Y, Segal M, Moses E (2016) Network synchronization in hippocampal neurons. *Proceedings of the National Academy of Sciences* 113(12):3341–3346.
18. Araque A, Carmignoto G, Haydon PG (2001) Dynamic signaling between astrocytes and neurons. *Annual review of physiology* 63(1):795–813.
19. Chever O, Dossi E, Pannasch U, Derangeon M, Rouach N (2016) Astroglial networks promote neuronal coordination. *Sci. Signal.* 9(410):ra6–ra6.
20. Haydon PG (2001) Glia: listening and talking to the synapse. *Nature Reviews Neuroscience* 2(3):185.
21. Hansson E, Rönnbäck L (2003) Glial neuronal signaling in the central nervous system. *The FASEB Journal* 17(3):341–348.
22. Pascual O, et al. (2005) Astrocytic purinergic signaling coordinates synaptic networks. *Science* 310(5745):113–116.
23. Verkhratsky A, Orkand RK, Kettenmann H (1998) Glial calcium: homeostasis and signaling function. *Physiological reviews* 78(1):99–141.
24. Araque A, Parpura V, Sanzgiri RP, Haydon PG (1999) Tripartite synapses: glia, the unacknowledged partner. *Trends in neurosciences* 22(5):208–215.
25. Rothstein JD, et al. (1996) Knockout of glutamate transporters reveals a major role for astroglial transport in excitotoxicity and clearance of glutamate. *Neuron* 16(3):675–686.
26. Coulter DA, Eid T (2012) Astrocytic regulation of glutamate homeostasis in epilepsy. *Glia* 60(8):1215–1226.
27. Tsodyks M, Uziel A, Markram H, , et al. (2000) Synchrony generation in recurrent networks with frequency-dependent synapses. *J Neurosci* 20(1):825–835.
28. Danbolt N, et al. (1998) Properties and localization of glutamate transporters in *Progress in brain research*. (Elsevier) Vol. 116, pp. 23–43.
29. Hertz L, Dringen R, Schousboe A, Robinson SR (1999) Astrocytes: glutamate producers for neurons. *Journal of neuroscience research* 57(4):417–428.
30. Murphy-Royal C, et al. (2015) Surface diffusion of astrocytic glutamate transporters shapes synaptic transmission. *Nature Neuroscience* 18:219–226.
31. Huang YT, Chang YL, Chen CC, Lai PY, Chan C (2017) Positive feedback and synchronized bursts in neuronal cultures. *PloS one* 12(11):e0187276.
32. Eytan D, Marom S (2006) Dynamics and effective topology underlying synchronization in networks of cortical neurons. *Journal of Neuroscience* 26(33):8465–8476.
33. Clements JD, Lester R, Tong G, Jahr CE, Westbrook GL (1992) The time course of glutamate in the synaptic cleft. *Science* 258(5087):1498–1501.
34. Bredt DS, Nicoll RA (2003) Ampa receptor trafficking at excitatory synapses. *Neuron* 40(2):361–379.
35. Lehre KP, Danbolt NC (1998) The number of glutamate transporter subtype molecules at glutamatergic synapses: chemical and stereological quantification in young adult rat brain. *Journal of Neuroscience* 18(21):8751–8757.
36. Eulenburg V, Gomeza J (2010) Neurotransmitter transporters expressed in glial cells as regulators of synapse function. *Brain research reviews* 63(1-2):103–112.
37. Kavalali ET, Klingauf J, Tsien RW (1999) Activity-dependent regulation of synaptic clustering in a hippocampal culture system. *Proceedings of the National Academy of Sciences* 96(22):12893–12900.
38. Marvin JS, et al. (2013) An optimized fluorescent probe for visualizing glutamate neurotransmission. *Nature methods* 10(2):162.
39. Armbruster M, Hanson E, Dulla CG (2016) Glutamate clearance is locally modulated by presynaptic neuronal activity in the cerebral cortex. *Journal of Neuroscience* 36(40):10404–10415.
40. Ziburkus J, Cressman JR, Barreto E, Schiff SJ (2006) Interneuron and pyramidal cell interplay during in vitro seizure-like events. *Journal of neurophysiology* 95(6):3948–3954.
41. Kudela P, Franaszczuk PJ, Bergey GK (2003) Changing excitation and inhibition in simulated neural networks: effects on induced bursting behavior. *Biological cybernetics* 88(4):276–285.
42. Chen C, Chen L, Lin Y, Zeng S, Luo Q (2006) The origin of spontaneous synchronized burst in cultured neuronal networks based on multi-electrode arrays. *Biosystems* 85(2):137–143.
43. Iida S, Shimba K, Sakai K, Kotani K, Jimbo Y (2018) Synchronous firing patterns of induced pluripotent stem cell-derived cortical neurons depend on the network structure consisting of excitatory and inhibitory neurons. *Biochemical and biophysical research communications* 501(1):152–157.
44. Lau PM, Bi GQ (2005) Synaptic mechanisms of persistent reverberatory activity in neuronal networks. *Proceedings of the National Academy of Sciences* 102(29):10333–10338.
45. Dani JW, Chernjavsky A, Smith SJ (1992) Neuronal activity triggers calcium waves in hippocampal astrocyte networks. *Neuron* 8(3):429–440.
46. Panatier A, et al. (2011) Astrocytes are endogenous regulators of basal transmission at central synapses. *Cell* 146(5):785–798.
47. Volman V, Gerkin RC, Lau PM, Ben-Jacob E, Bi GQ (2007) Calcium and synaptic dynamics underlying reverberatory activity in neuronal networks. *Physical biology* 4(2):91.
48. Huang CH, Huang YT, Chen CC, Chan C (2017) Propagation and synchronization of reverberatory bursts in developing cultured networks. *Journal of computational neuroscience* 42(2):177–185.
49. Jabaudon D, et al. (1999) Inhibition of uptake unmasks rapid extracellular turnover of glutamate of nonvesicular origin. *Proceedings of the National Academy of Sciences* 96(15):8733–8738.
50. Bacci A, et al. (2002) Block of glutamate-glutamine cycle between astrocytes and neurons inhibits epileptiform activity in hippocampus. *Journal of Neurophysiology* 88(5):2302–2310.

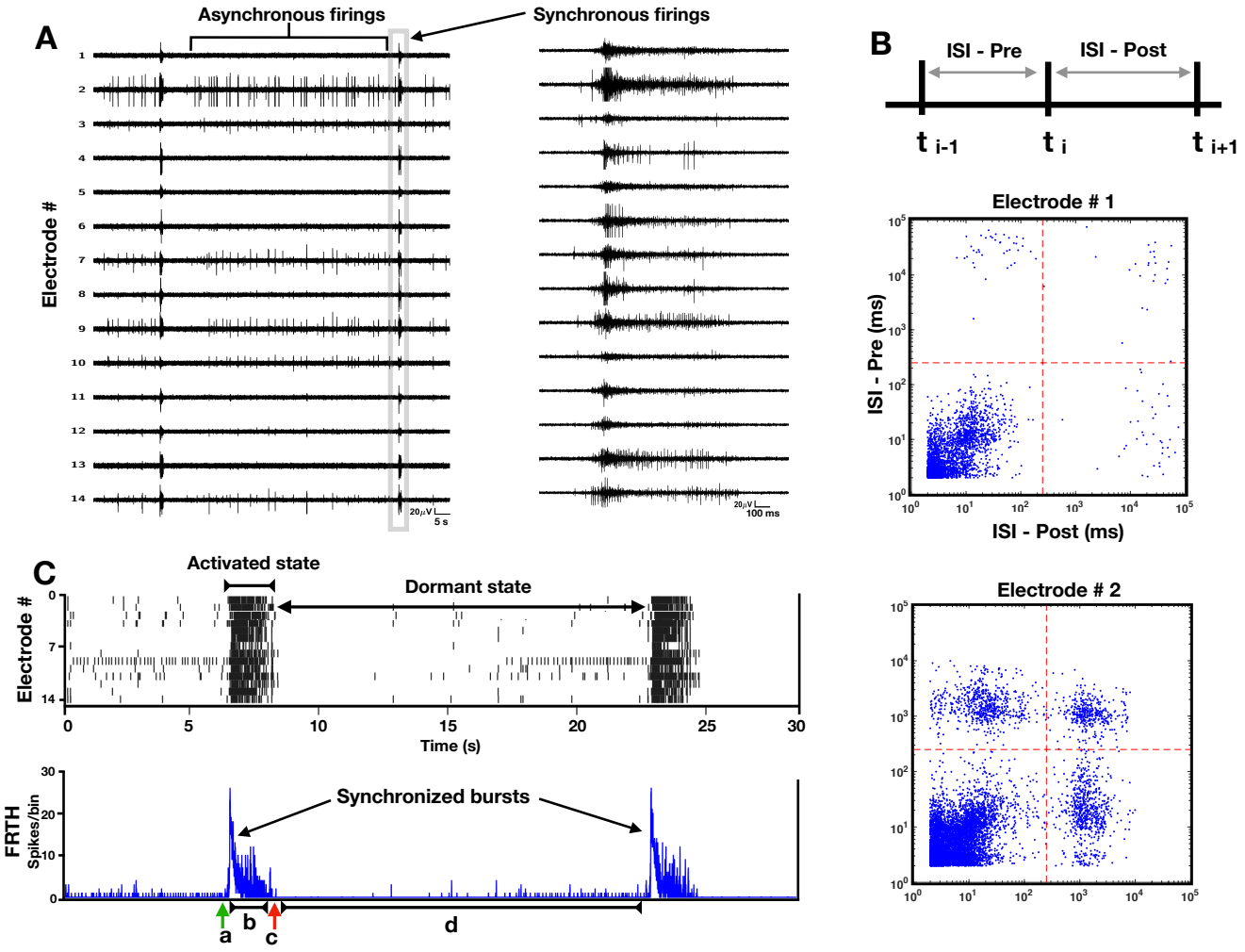

Fig. 1. Activated and dormant states of neurons in cortical cultures

(A) Time series of extracellular field potentials of a sample cortical network, recorded with 14 electrodes using a multi-electrode array probe. Spontaneous electrical activities of cortical neurons in a developing network (22 days *in vitro*) appear as asynchronous or synchronous firings. (B) A inter-spike interval (ISI) distribution, generated by plotting time intervals (top) between successive firings, show a distinction between synchronous and asynchronous firing events. Electrode#1 engaging only in synchronous firings exhibit only one dense cluster of ISI lying in 2–100 ms range (middle), while the electrode#2 also engaging in asynchronous firings show additional ISI clusters lying above 1 sec region (bottom). (C) Raster plot of detected spikes (top, black trace) illustrates two states of network in general: 'activated' state when all units exhibit synchronous burst (SB) firings followed by a 'dormant' state in which most units show no to very few activities. Corresponding firing-rate time histogram (FRTH) (bottom trace in blue), calculated by summing all the detected spikes within 5 ms bin size, displays the kinetic structure of network's states. The kinetics involve an initiation (a), maintenance (b), and termination (c) phases followed by a much longer dormant phase (d).

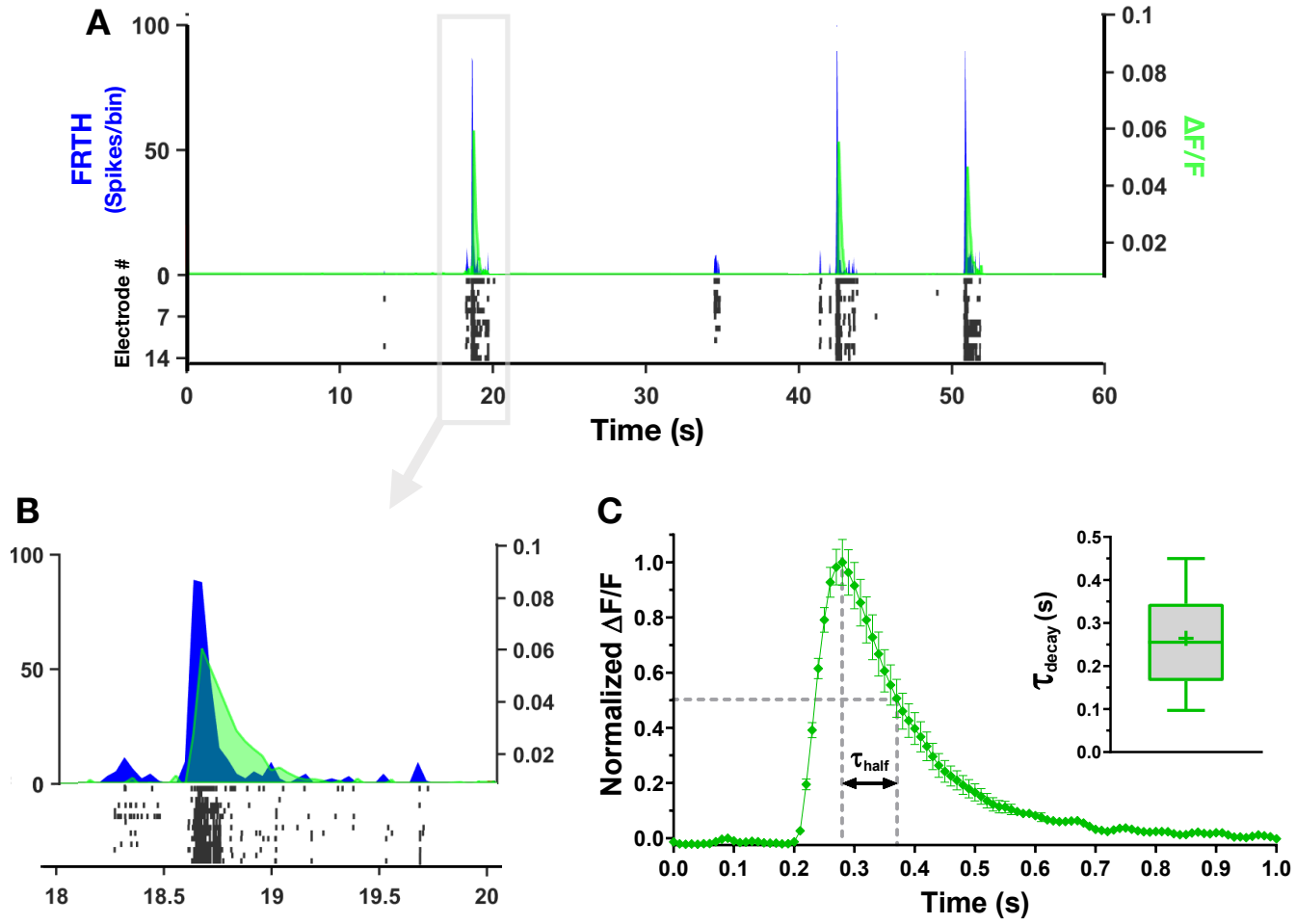

Fig. 2. Synaptic glutamate level rises and falls during SBs

Simultaneous recording of neuronal activities with MEA and synaptic glutamate dynamics detected by astrocytes with iGluSnFr imaging. (A) Top panel shows summed neuronal spiking activities as firing-rate time histogram (FRTH with bin size 40ms, blue trace) overlapped with glutamate dynamics detected simultaneous through iGluSnFr imaging. Change in fluorescence is plot as $\Delta F/F$ (green trace). Bottom raster plot (black) shows detected neuronal activities from individual electrodes. (B) shows enlarged view of one of the SB events in A. Note that synaptic glutamate level increases globally and decays rapidly during and after SB events. (C) Average normalized fluorescence $\Delta F/F$ from a sample network (green trace). The time taken for decrease of synaptic glutamate level from its maximum to half during SB is denoted by τ_{half}. Inset, summary of glutamate decay time τ_{decay} in cultured cortical networks, calculated as $\tau_{\text{half}}/\ln 2$. Middle line in the box plot shows median and cross represents mean(0.26±0.11 s, n=8 cultures).

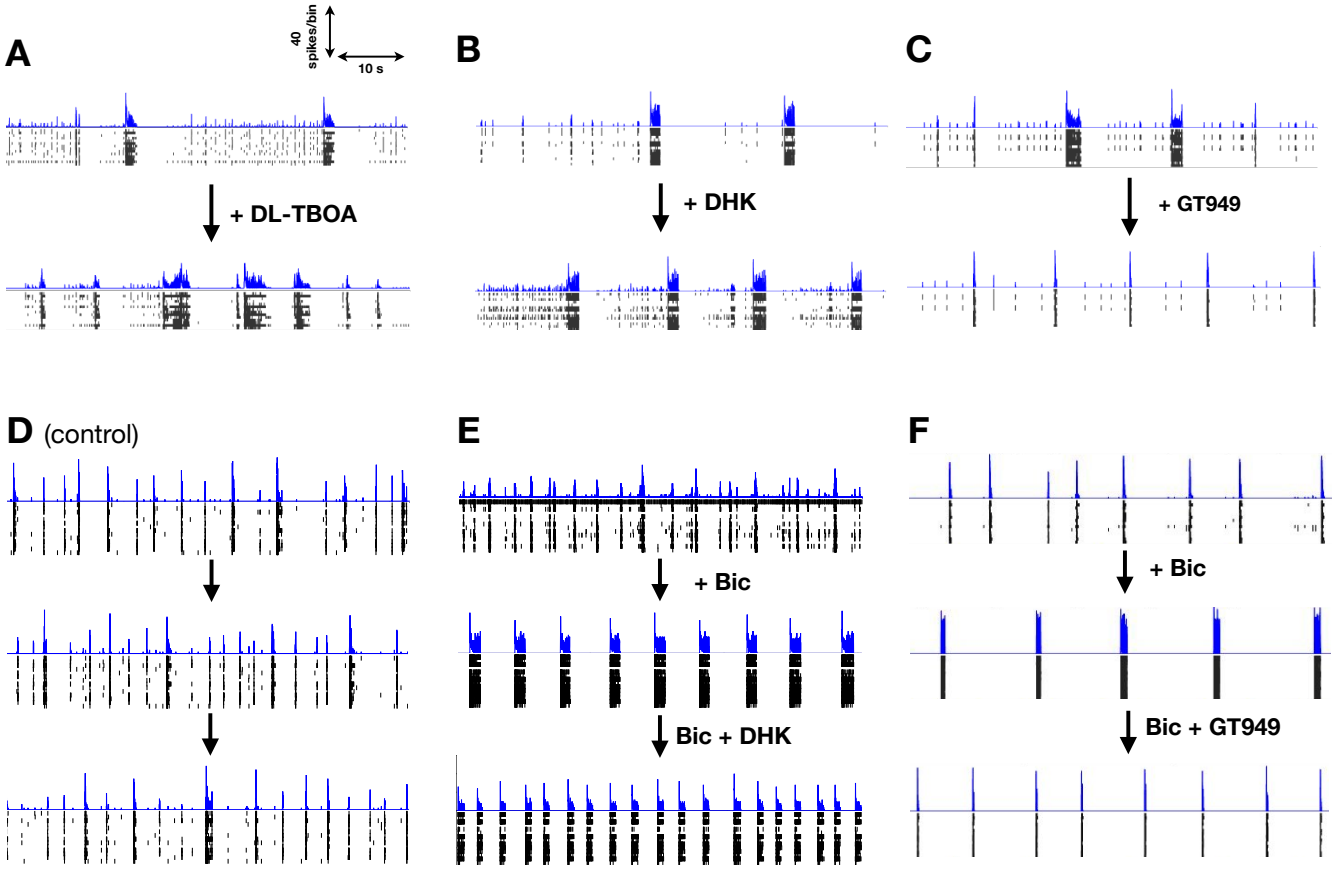

Fig. 3. Pharmacological manipulation of glutamate transporters alters SB dynamics

Figures(A–F) shows one-minute snapshots of firing activities obtained from six different cortical networks. FRTHs generated with a bin size of 5ms are shown in blue while the corresponding raster plot of detected spikes are shown in black. The interval between each snapshot of a network, shown in the order as indicated by the arrow marks, were at least separated by 45 minutes. The first snapshot of each network shows its reference activities level. Network in D shows the time effect on network dynamics in a long duration recording. Without any pharmacological treatment network maintained similar firing and bursting patterns over a period of 120 minutes. Network in A, after treatment with DL-TBOA (10μM), resulted in prolonged and frequent SBs. The dormant states were shorter and contained with lesser asynchronous activities. Similar effects were observed after DHK (GLT-1 specific, 200μM) treatment in network in B. The only difference between DHK and DL-TBOA was an increase of asynchronous activities during the dormant state under DHK. Specific augmentation of GLT-1 (10μM) of network in C with GT949 resulted in shortening of SBs. GLT-1's role was further tested in disinhibited state of cortical networks. Without any drug addition, network in D showed similar firing and bursting patterns at the different intervals. Disinhibition with bicuculline (Bic, GABA inhibitor, 10μM), shown in network in E, resulted in more robust SB patterns with clear activated and dormant states of network. Resulting SBs were longer than reference. Further DHK (200μM) addition, enhanced SB frequency and reduced SB duration at the same time. Enhancing GLT-1 function with GT949 (10μM) treatment in disinhibited state (network in F), resulted in shorter SBs.

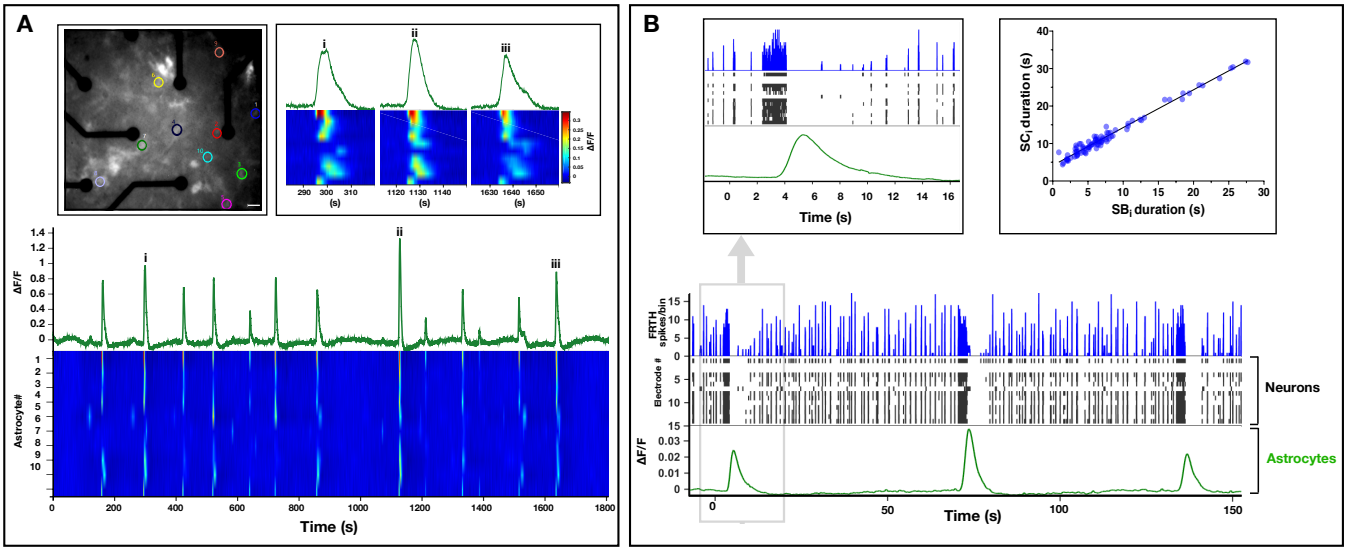

Fig. 4. Astrocytes exhibit synchronous calcium dynamics following SBs

(A)Top inset on left shows fluorescence micro-graph of a culture expressed with cyto-GCaMP6f calcium sensors in astrocytes, scale bar – 30 μm. Different colored circles indicate locations of 10 randomly selected and spatially distant calcium-active astrocytes. Traces in green show summed fluorescence intensity–time plot of the selected astrocytes. Heatmap shows corresponding temporal dynamics of calcium intensity in individual astrocytes. Top right inset shows enlarged view of three synchronous calcium elevation (SCE) events marked as (i,ii,ii). Note that the activation pattern remains similar in each event, indicating a hierarchical order of astrocyte activation during SCEs. (B) Shows temporally aligned activities of neurons obtained from MEA (FRTH with 40 ms bin size, blue trace) and corresponding raster plot(black trace), with collective calcium activities in astrocytes. Top left inset, shows enlarged view of a global event when an astrocytic SCE appears after a long persisting neuronal SB. Note that all neuronal activities ceased during the global calcium rise in astrocytes. Neuronal activity reappeared soon after the SCE decay. (Top left inset) Duration of SCE was found to be linearly related to its preceding SB duration($n = 87$, 4 cultures).

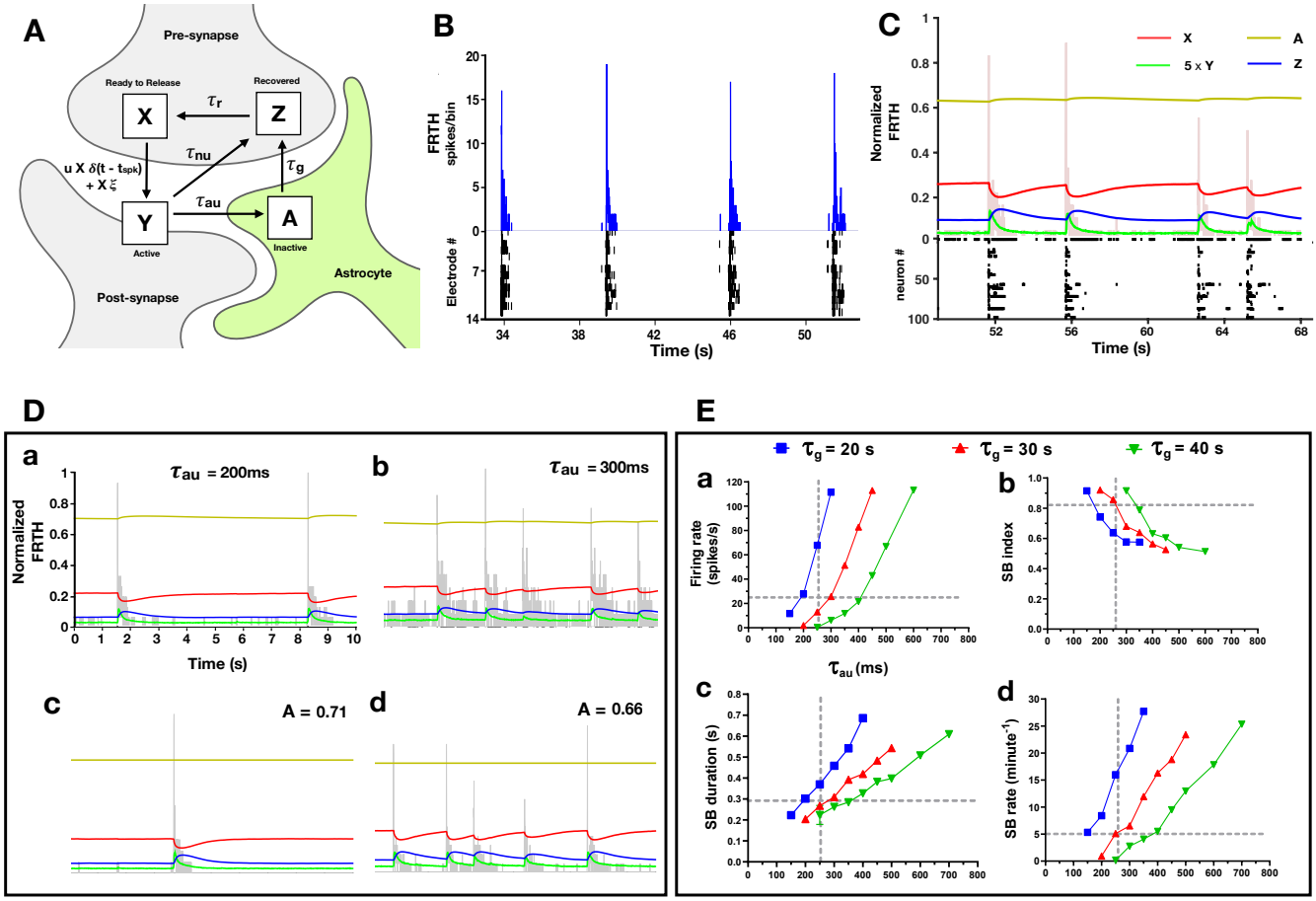

Fig. 5. Simulation with TUMA synapses reproduces experimental observations

(A)Schematic representation of TUMA, tripartite synapse model describing glutamate recycling. The fraction of the total amount of the glutamate in these various states are represented by X (in presynapse), Y(at synapse), Z(recovered at presynapse) and A(in astrocytes) as shown in the figure and $X + Y + Z + A = 1$. Impulses $\delta(t - t_{\rm spk})$ created by spikes at time $t = t_{\rm spk}$, arriving at the presynapse, trigger glutamate release into the cleft. Released glutamate molecules rapidly activate the post synaptic fast receptors until their clearance by neuronal and astrocytic uptake with timescales $\tau_{\rm nu}$ and $\tau_{\rm au}$ respectively. The astrocytic uptake follows glutamate–glutamine cycle leading to slow recovery of glutamate at the timescale of τ_g in the presynapse. Once recovered, glutamate gets packed into vesicles and retrieved back at the active zone within τ_r. During this recovery process, some neurons may exhibit noise(ξ) induced asynchronous release. (B) Shows FRTH (blue trace, bin size 5ms) and raster plot (black trace) of neuronal activities obtained from MEA. (C) Similar firing and bursting patterns were obtained from simulation (random network of 100 neurons connected with TUMA synapses). Simulated normalized FRTH trace (bin size 5ms) is overlapped with the four-state X(red), Y(green), Z(blue), and A(yellow) dynamics of glutamate occurring simultaneously in the network. These traces denotes the average fraction of glutamate distributed around synapse. For visual clarity, Y is shown 5 times its actual values. (D) Effects of varying the astrocytic uptake timescale on network firing patterns(FRTH, gray trace). Subplots D(b–d) share the same vertical and horizontal axis scales with D(a). Increasing $\tau_{\rm au}$ from 200 ms to 300 ms resulted in longer and frequent SBs similar to DHK effects.(D,c–d) By fixing A to the mean values (0.71 and 0.66) obtained from $\tau_{\rm au}$ (200 and 300ms) did not affect the SB patterns.(E) Summary of network firing statistics dependence on astrocytic uptake rate $\tau_{\rm au}$ and transport τ_g. Each data point represents the mean value obtained at the specified parameter values. Effects of varying τ_g, i.e., recovery time of glutamate from astrocytes is shown in color-coded traces. Overlapped vertical and horizontal broken gray lines represent the approximate mean value of glutamate decay time ($\tau_{\rm decay}$ analogue for astrocytic glutamate uptake, $\tau_{\rm au}$) obtained from experiment (Figure 2C) and the approximate SB statistical mean values obtained from MEA data analysis respectively. The simulated firing and SB statistics were found to match with experimental observations when τ_g was close to 30s.

51. Tani H, et al. (2014) A local glutamate-glutamine cycle sustains synaptic excitatory transmitter release. *Neuron* 81(4):888–900.
52. Taschenberger H, Scheuss V, Neher E (2005) Release kinetics, quantal parameters and their modulation during short-term depression at a developing synapse in the rat cns. *The Journal of physiology* 568(2):513–537.
53. Hardingham NR, et al. (2010) Quantal analysis reveals a functional correlation between presynaptic and postsynaptic efficacy in excitatory connections from rat neocortex. *Journal of Neuroscience* 30(4):1441–1451.
54. Budisantoso T, et al. (2013) Evaluation of glutamate concentration transient in the synaptic cleft of the rat calyx of held. *The Journal of physiology* 591(1):219–239.
55. Montana V, Malarkey EB, Verderio C, Matteoli M, Parpura V (2006) Vesicular transmitter release from astrocytes. *Glia* 54(7):700–715.
56. Zhang Jm, et al. (2003) Atp released by astrocytes mediates glutamatergic activity-dependent heterosynaptic suppression. *Neuron* 40(5):971–982.
57. Mehta B, Begum G, Joshi NB, Joshi PG (2008) Nitric oxide–mediated modulation of synaptic activity by astrocytic p2y receptors. *The Journal of general physiology* 132(3):339–349.
58. Parpura V, Haydon PG (2000) Physiological astrocytic calcium levels stimulate glutamate release to modulate adjacent neurons. *Proceedings of the National Academy of Sciences* 97(15):8629–8634.
59. Tanaka K, et al. (1997) Epilepsy and exacerbation of brain injury in mice lacking the glutamate transporter glt-1. *Science* 276(5319):1699–1702.
60. Werner P, Pitt D, Raine CS (2001) Multiple sclerosis: altered glutamate homeostasis in lesions correlates with oligodendrocyte and axonal damage. *Annals of neurology* 50(2):169–180.
61. Bechtholt-Gompf AJ, et al. (2010) Blockade of astrocytic glutamate uptake in rats induces signs of anhedonia and impaired spatial memory. *Neuropsychopharmacology* 35(10):2049.
62. Scofield MD, Kalivas PW (2014) Astrocytic dysfunction and addiction: consequences of impaired glutamate homeostasis. *The Neuroscientist* 20(6):610–622.
63. John CS, et al. (2012) Blockade of astrocytic glutamate uptake in the prefrontal cortex induces anhedonia. *Neuropsychopharmacology* 37(11):2467.
64. Harada K, Kamiya T, Tsuboi T (2016) Gliotransmitter release from astrocytes: functional, developmental and pathological implications in the brain. *Frontiers in neuroscience* 9:499.